


 Cite this: *RSC Adv.*, 2023, **13**, 19265

# Simultaneous nitrate and sulfate biotransformation driven by different substrates: comparison of carbon sources and metabolic pathways at different C/N ratios†

 Baixiang Wang,<sup>a</sup> Heping Hu,<sup>b</sup> Shaobin Huang,<sup>ID \*a</sup> Haiguang Yuan,<sup>a</sup> Yanling Wang,<sup>a</sup> Tianyu Zhao,<sup>a</sup> Zerui Gong<sup>a</sup> and Xinyue Xu<sup>a</sup>

Nitrate ( $\text{NO}_3^-$ ) and sulfate ( $\text{SO}_4^{2-}$ ) often coexist in organic wastewater. The effects of different substrates on  $\text{NO}_3^-$  and  $\text{SO}_4^{2-}$  biotransformation pathways at various C/N ratios were investigated in this study. This study used an activated sludge process for simultaneous desulfurization and denitrification in an integrated sequencing batch bioreactor. The results revealed that the most complete removals of  $\text{NO}_3^-$  and  $\text{SO}_4^{2-}$  were achieved at a C/N ratio of 5 in integrated simultaneous desulfurization and denitrification (ISDD). Reactor Rb (sodium succinate) displayed a higher  $\text{SO}_4^{2-}$  removal efficiency (93.79%) with lower chemical oxygen demand (COD) consumption (85.72%) than reactor Ra (sodium acetate) on account of almost 100% removal of  $\text{NO}_3^-$  in both Ra and Rb. Ra produced more  $\text{S}^{2-}$  (5.96 mg L<sup>-1</sup>) and  $\text{H}_2\text{S}$  (25 mg L<sup>-1</sup>) than Rb, which regulated the biotransformation of  $\text{NO}_3^-$  from denitrification to dissimilatory nitrate reduction to ammonium (DNRA), whereas almost no  $\text{H}_2\text{S}$  accumulated in Rb which can avoid secondary pollution. Sodium acetate-supported systems were found to favor the growth of DNRA bacteria (*Desulfovibrio*); although denitrifying bacteria (DNB) and sulfate-reducing bacteria (SRB) were found to co-exist in both systems, Rb has a greater keystone taxa diversity. Furthermore, the potential carbon metabolic pathways of the two carbon sources have been predicted. Both succinate and acetate could be generated in reactor Rb through the citrate cycle and the acetyl-CoA pathway. The high prevalence of four-carbon metabolism in Ra suggests that the carbon metabolism of sodium acetate is significantly improved at a C/N ratio of 5. This study has clarified the biotransformation mechanisms of  $\text{NO}_3^-$  and  $\text{SO}_4^{2-}$  in the presence of different substrates and the potential carbon metabolism pathway, which is expected to provide new ideas for the simultaneous removal of  $\text{NO}_3^-$  and  $\text{SO}_4^{2-}$  from different media.

 Received 25th April 2023  
 Accepted 20th June 2023

 DOI: 10.1039/d3ra02749j  
[rsc.li/rsc-advances](http://rsc.li/rsc-advances)

## 1 Introduction

Nitrate ( $\text{NO}_3^-$ ) and sulfate ( $\text{SO}_4^{2-}$ ) are often found in waste streams of mariculture, resin regeneration, and food processing.<sup>1-3</sup> Nitrate in sewage wastewater not only contributes to climate change, but also to eutrophication of water bodies and loss of biodiversity. The sulfide produced in the process of sulfate conversion is toxic and seriously pollutes the environment. Currently, various methods for removing  $\text{NO}_3^-$  and  $\text{SO}_4^{2-}$  are recommended, including ion-exchange, adsorption, reverse osmosis, biological denitrification, and electrodialysis.<sup>4,5</sup> Among them, the biological technique can reduce  $\text{NO}_3^-$  and  $\text{SO}_4^{2-}$  to nitrogen and elemental sulfur with no secondary pollution and minimal operating expenses.<sup>6</sup>  $\text{NO}_3^-$  can be

biologically transformed to dinitrogen ( $\text{N}_2$ ) gas by denitrification through heterotrophic and/or autotrophic pathways. Different from denitrification, dissimilatory nitrate reduction to ammonium (DNRA) reduced  $\text{NO}_3^-$  to ammonium ( $\text{NH}_4^+$ ) via  $\text{NO}_2^-$  under anaerobic conditions, so that all inorganic nitrogen in the water existed in the sole form of  $\text{NH}_4^+$ . Sulfate-reducing bacteria (SRB) can anaerobically reduce  $\text{SO}_4^{2-}$  to sulfide ( $\text{S}^{2-}$ ) at the expense of chemical oxygen demand (COD).<sup>7</sup>

The simultaneous removal of  $\text{NO}_3^-$  and  $\text{SO}_4^{2-}$  in a single bioreactor would be beneficial for wastewater treatment since it would streamline the technical process flow and reduce operating costs. However, it is very challenging to achieve efficient integrated simultaneous desulfurization and denitrification (ISDD) in a single reactor without secondary pollution owing to the intense competition between different groups of bacteria. The simultaneous reduction of  $\text{NO}_3^-$  and  $\text{SO}_4^{2-}$  requires the successful integration of several potential microbial reaction pathways, including denitrification, DNRA, desulfurization, and sulfide oxidation. It is difficult to control the effective dissolved

<sup>a</sup>South China University of Technology, China. E-mail: chshuang@scut.edu.cn

<sup>b</sup>China Water Resources Pearl River Planning Surveying & Designing Co. Ltd, China

† Electronic supplementary information (ESI) available. See DOI: <https://doi.org/10.1039/d3ra02749j>



oxygen (DO) level in the reactor due to the different environmental ecological niches of keystone taxa involved in the system, and maintaining DO in the range  $0.10\text{--}0.12\text{ mg L}^{-1}$  remains a technical challenge requiring additional energy and cost.<sup>8</sup> Due to the dissolved oxygen (DO) concentration gradient in the SBR plant, the DO concentration is higher in the upper part of the plant, where sulfide is converted to sulfur. On the one hand, the presence of nitrate can inhibit the release of hydrogen sulfide by promoting the competition of nitrate-reducing bacteria for substrate to inhibit the growth of sulfate-reducing microorganisms.<sup>9</sup> On the other hand, nitrite intermediates produced during denitrification can inhibit the release of hydrogen sulfide by inhibiting the further reduction of sulfite through biological inhibition of functional enzymes involved in the sulfur reduction process.<sup>10</sup> However, it has also been shown that the addition of nitrate stimulates sulfide oxidation-nitrate reduction microorganisms in the microenvironment and does not only inhibit the enzymatic activity associated with sulfate related microorganisms.<sup>11</sup> Competition between various electron acceptors is driven by DO at different C/N ratios. The success of simultaneous degradation of  $\text{SO}_4^{2-}$ ,  $\text{NO}_3^-$ , and organic carbon depends on the synergistic growth of autotrophic and heterotrophic denitrifying bacteria. Xu *et al.*<sup>12</sup> investigated the interactions between SRB, sulfide oxidation bacteria (SOB), heterotrophic nitrate reducing bacteria (hNRB), and autotrophic nitrate reducing bacteria (aNRB) under denitrifying sulfide removal (DSR) conditions. They noted that  $\text{S}^{2-}$  oxidation by aNRB proceeded at only half the rate with nitrite ( $\text{NO}_2^-$ ) as an electron acceptor than with  $\text{NO}_3^-$ . The reduction rate of  $\text{NO}_3^-$  by aNRB was also shown to be much slower than when using  $\text{S}^0$  as an electron donor.<sup>7</sup> Ontiveros-Valencia *et al.*<sup>13</sup> indicated that SRB are only able to initiate strong sulfate reduction (SR) when competition for electron donors within a biofilm is relieved by near-complete removal of  $\text{NO}_3^-$  under all conditions tested.  $\text{NO}_3^-$  serves as a key factor in controlling the shift of SR and DSR, while the C/N ratio directly influences the process of SR in the system.<sup>8</sup> In general, high C/N ratio ( $>2.25$ ) in an ISDD system favors the removal of  $\text{NO}_3^-$ ,<sup>14</sup> while SR is inhibited. Chen *et al.*<sup>15</sup> also noted that with increasing C/N ratio in a solution, SR becomes inhibited. Feeding wastewaters at high C/N ratio would stimulate overgrowth of heterotrophic bacteria in the reactor, thereby suppressing the growth of aNRB.<sup>16</sup> In addition, the inhibition of SR by  $\text{NO}_3^-$  is due in part to  $\text{NO}_3^-$  reduction,  $\text{S}^{2-}$  oxidation processes, the preferential affinity of some SRB for  $\text{NO}_3^-$  as an electron acceptor, and prevention of the effects of reduced  $\text{NO}_2^-$  on SRB metabolism.<sup>4</sup> Therefore, it is necessary to investigate the effect of carbon sources on microbial communities for nitrogen and sulfur removal at different C/N ratios.

In  $\text{NO}_3^-$  and  $\text{SO}_4^{2-}$  removal, the keystone taxa are affected by different carbon sources. Carlson *et al.*<sup>9</sup> have demonstrated that  $\text{NO}_3^-$  can inhibit SRB activity through both bio-competitive exclusion and outgrowth of hNRB. Previous research has revealed that *Pseudomonas* and *Azoarcus* are enriched when using acetate as the carbon source, and succinate has been identified as the optimal carbon source for *Pseudomonas aeruginosa* and *Pseudomonas putida*.<sup>17</sup> It has

been shown that in systems involving simultaneous denitrification and DNRA, the DNRA bacteria are enriched when using acetate as the carbon source,<sup>18</sup> the dominant DNRA microorganisms are *Thauera* and *Geobacter*. Some other slightly more complex species, such as D-cellulose, are favored to enrich *Enterobacter* and *Pseudomonas* genera in low secondary salinized soil.<sup>19</sup> The utilization of acetate as an electron donor is preferred for the denitrification of highly concentrated  $\text{NO}_3^-$  waste.<sup>20</sup> However, Cai *et al.*<sup>4</sup> found that SRB showed lower activity with acetate than with propionate. In a reactor with complex carbon sources, microorganisms show strong competition for these carbon sources, but there are insufficient electron donors to drive multiple reactions. In a relatively simple carbon source environment, even if microorganisms compete for carbon sources, there will be sufficient carbon sources as electron donors to drive the relevant reactions.<sup>21</sup> Since succinate and acetate are the basic substances in the carbon metabolism pathway, succinic acid is present in the Citrate cycle and acetate is present in the acetyl CoA pathway, therefore, acetate and succinate were chosen as carbon sources for this study. Nevertheless, the reactions involved in simultaneous  $\text{NO}_3^-$  and  $\text{SO}_4^{2-}$  removal in the presence of various carbon sources and the potential microbial metabolic pathways involving carbon, nitrogen, and sulfur have yet to be fully delineated.

To explore how microbial communities shaped by different carbon sources and C/N ratios alter their carbon metabolism pathways to achieve efficient simultaneous removal of  $\text{NO}_3^-$  and  $\text{SO}_4^{2-}$ , and the general patterns for the response of an ISDD system to different substrates, acetate and succinate were selected as additional carbon sources in this study. Batch experiments were carried out to identify differences in the intermediates produced with the respective substrates. Furthermore, EEM and 16S rRNA have been applied to determine the type of organic matter and the microbial phylogeny of functional communities in the relevant reactors.

## 2 Experimental

### 2.1. Reactor set-up and operation

Measurements were performed with different carbon sources in two identical mixed batch reactors (designated as Ra and Rb), which have been operated for more than a year with consistent stable performance, to investigate the effects of acetate and succinate, respectively. Ra and Rb were operated in parallel in three consecutive stages at various C/N ratios of 8 : 1 (stage 1, operation for 20 days), 5 : 1 (stage 2, operation for 20 days), and 3 : 1 (stage 3, operation for 20 days). The set-up is shown in Fig. 1. The operating volume was 1800 mL with physical stirring (100 rpm) and a thermostatic control unit maintained the temperature at  $30 \pm 1^\circ\text{C}$ . A proportion of 25% of the total liquid volume was exchanged as required by means of an automatic drainage unit. The hydraulic retention time (HRT) was 24 h, including 23.5 h of agitation and 0.5 h of setting and drainage in each sequencing batch reactor cycle. Operating parameters are detailed in Table S1.†



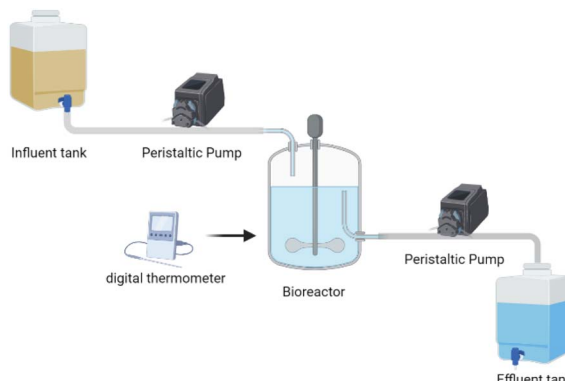


Fig. 1 Schematic diagram of the reactor set-up.

## 2.2. Synthetic wastewater and active sludge

Reactors Ra and Rb were loaded with sodium acetate and sodium succinate, respectively. The following components were used to create the synthetic input media at different stages: Ra: sodium acetate 3.41/2.13/1.28 g L<sup>-1</sup>; Rb: disodium succinate 3.38/2.10/1.26 g L<sup>-1</sup>. The other components in the two reactors were the same: Na<sub>2</sub>SO<sub>4</sub> 1.48 g L<sup>-1</sup>, KNO<sub>3</sub> 1.05 g L<sup>-1</sup>, NaHCO<sub>3</sub> 0.60 g L<sup>-1</sup>, KH<sub>2</sub>PO<sub>4</sub> 0.22 g L<sup>-1</sup>, CaCl<sub>2</sub> 0.1 g L<sup>-1</sup>, MgCl<sub>2</sub> 0.1 g L<sup>-1</sup>, and 1 mL L<sup>-1</sup> trace element solution.<sup>22</sup> Lijiao Wastewater Treatment Plant in Guangzhou provided the anaerobic activated sludge of Secondary sedimentation tank that was used to inoculate the bioreactor.

## 2.3. Batch experiments

After two months of trials at different C/N ratios, experiments were conducted at a C/N ratio of 5 to further observe the nitrogen to sulfur conversions with different carbon sources. Before the test, the denitrifying biomass was washed three times with phosphate buffered saline (PBS) to ensure that no original nutrient solution remained. Subsequently, a mixture of activated sludge and fresh nutrient solution in a ratio of 1:10 (v/v) was placed in a 250 mL conical flask and incubated at 30 °C with stirring at 100 rpm in anoxic condition. The composition of the nutrient solution was the same as above for a C/N ratio of 5: Ra: sodium acetate 2.13 g L<sup>-1</sup>; Rb: disodium succinate 2.10 g L<sup>-1</sup>; Na<sub>2</sub>SO<sub>4</sub> 1.48 g L<sup>-1</sup>, KNO<sub>3</sub> 1.05 g L<sup>-1</sup>, NaHCO<sub>3</sub> 6.0 g L<sup>-1</sup>, KH<sub>2</sub>PO<sub>4</sub> 0.22 g L<sup>-1</sup>, CaCl<sub>2</sub> 0.1 g L<sup>-1</sup>, and MgCl<sub>2</sub> 0.1 g L<sup>-1</sup>. Aliquots (10 mL) were withdrawn at intervals of 3 h over the 24 h duration of the experiment, immediately passed through a 0.45 µm filter membrane, and then promptly frozen at -4 °C for follow-up tests. Variations in COD, oxidation-reduction potential (ORP), NH<sub>4</sub><sup>+</sup>, NO<sub>3</sub><sup>-</sup>, NO<sub>2</sub><sup>-</sup>, SO<sub>4</sub><sup>2-</sup>, S<sup>2-</sup>, H<sub>2</sub>S, and N<sub>2</sub>O were measured during the experiment.

## 2.4. Analysis methods and calculation

DO, pH, ORP, temperature, and NO<sub>3</sub><sup>-</sup> concentration were measured according to a previously established procedure.<sup>23</sup> A microplate reader was used to spectrophotometrically quantify NH<sub>4</sub><sup>+</sup>, NO<sub>2</sub><sup>-</sup>, S<sup>2-</sup>, and COD (EPOCH-2; BioTek, Winooski, VT, USA). SO<sub>4</sub><sup>2-</sup>, SO<sub>3</sub><sup>2-</sup>, and S<sub>2</sub>O<sub>3</sub><sup>2-</sup> were measured by ion

chromatography (ICS-900; Dionex, Sunnyvale, CA, USA). Total dissolved H<sub>2</sub>S and N<sub>2</sub>O concentrations were measured using an array of microsensor multimeters (Unisense Co., Denmark). The organics in the reactors were determined by EEM fluorescence spectroscopy (F-7000 FL spectrophotometer).

The removal efficiencies of NO<sub>3</sub><sup>-</sup>, COD, and SO<sub>4</sub><sup>2-</sup> were calculated from the ratio of the difference in substrate concentration between the initial and effluent solutions to the initial substrate concentration.

$$RE_s = ([\text{substrate}]_{\text{inf}} - [\text{substrate}]_{\text{eff}})/[\text{substrate}]_{\text{inf}} \times 100\% \quad (1)$$

S<sup>0</sup> concentration was calculated by sulfur balance.

$$\begin{aligned} S^0 = & [SO_4^{2-} - S]_{\text{inf}} - [SO_4^{2-} - S]_{\text{eff}} - 2 \\ & \times [S_2O_3^{2-} - S]_{\text{eff}} - [SO_3^{2-} - S]_{\text{eff}} \\ & - [S^{2-} - S]_{\text{eff}} - [H_2S_{\text{aq/g}} - S]_{\text{eff}} \end{aligned} \quad (2)$$

## 2.5. DNA extraction and amplification, and 16S rRNA gene amplicon sequencing

Aliquots (5 mL) of activated sludge from reactors Ra and Rb, operating under various conditions, were taken in order to conduct a more thorough investigation into the effects on the microbial community. We used 338F (5'-ACTCCTACGGGAGGCAGCAG-3') and 806R (5'-GGACTTACHVGGGTWTCTAAT-3') sequences for PCR amplification of the V3-V4 region of the 16S rRNA gene. The Illumina MiSeq PE 300 platform (Majorbio Bio-Pharm Technology Co., Ltd, Shanghai, China) was utilized for the sequencing process. Fastp (<https://github.com/OpenGene/fastp>, version 0.20.0) software was used for further quality assurance of the initially obtained sequence, FLASH (<http://www.ccb.umd.edu/software/flash>, version 1.2.7) software was used for splicing, UPARSE software (<http://drive5.com/uparse/>, version 7.1) to accomplish OUT sequence grouping based on 97% similarity and to eliminate chimeras, and RDP classifier (<http://rdp.cme.msu.edu/>, version 2.2) to sort and annotate each sequence.

## 3 Results and discussion

### 3.1. General performances

The transformation performances with regard to NO<sub>3</sub><sup>-</sup> and SO<sub>4</sub><sup>2-</sup> reductions and COD removal of reactors Ra and Rb are depicted in Fig. 2(a) and (b). The experiments were conducted with different carbon sources at various C/N ratios, taking samples daily.

At C/N = 8, the NO<sub>3</sub><sup>-</sup> removal efficiency in reactor Ra was steadily at 98.01%, and that in reactor Rb was 99.45%. Somewhat unexpectedly, NH<sub>4</sub><sup>+</sup> was produced in Ra. Previous studies have demonstrated that the DNRA pathway is preferred at high C/N ratios.<sup>18</sup> Consequently, we envisage the DNRA pathway to be operative in reactor Ra, converting NO<sub>3</sub><sup>-</sup> into NH<sub>4</sub><sup>+</sup> in stage 1. The production of NH<sub>4</sub><sup>+</sup> in Rb was significantly less than that in Ra. Zhao *et al.* indicated that carbon sources with low numbers of carbon atoms are more amenable to the DNRA process.<sup>24</sup> Removals of SO<sub>4</sub><sup>2-</sup> were above 80% and 78% in Ra and Rb, respectively, in stage 1.



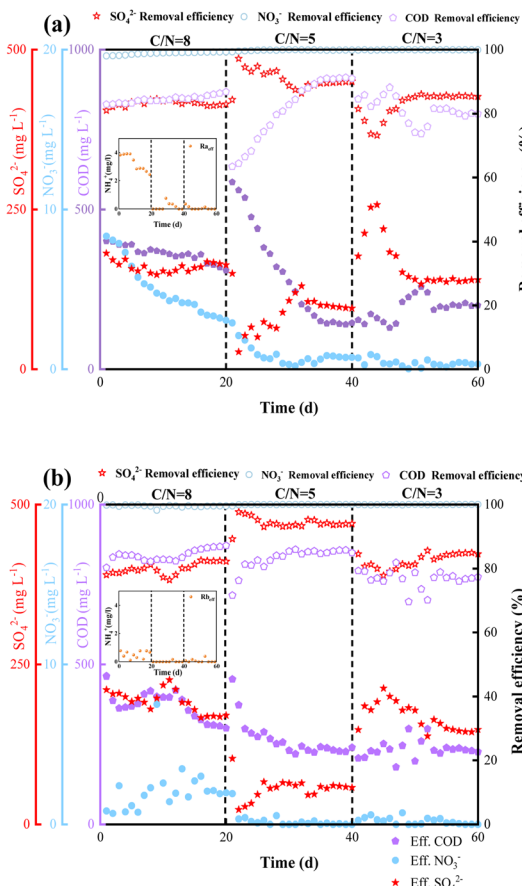


Fig. 2 Concentrations of  $\text{SO}_4^{2-}$ ,  $\text{NO}_3^-$ ,  $\text{NH}_4^+$ , and COD in effluent;  $\text{SO}_4^{2-}$ ,  $\text{NO}_3^-$ , and COD removal efficiencies of the two reactors during long-time reactor operation: (a) using sodium acetate as carbon source; (b) using sodium succinate as carbon source.

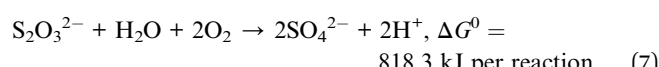
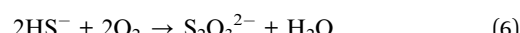
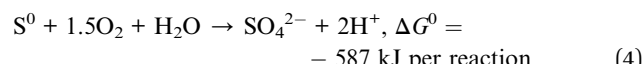
After day 20, the C/N ratio was reduced to 5. In the early stages of this period, the COD removal efficiency in Ra was maintained. The  $\text{SO}_4^{2-}$  reduction efficiency decreased, while remained higher than that in stage 1. We further observed that the COD removal efficiency was inversely proportional to the  $\text{SO}_4^{2-}$  removal efficiency. Hu *et al.*<sup>25</sup> reported that as COD/ $\text{SO}_4^{2-}$  decreased from 20 to 0.5, there was an increase in the efficiency of electron utilization by SRB from 3.5% to 20.6% in the competition between methane-producing archaea (MPA) and SRB. Moreover, SR in Rb (93.80%) was greater than that in Ra (89.85%). As for COD removal, the removal capacities in reactors Ra and Rb were both above 80%. SR and COD removal efficiency were highest at this stage, while the  $\text{NO}_3^-$  removal efficiency remained at a constant high level (>99%).

In phase 3 (C/N = 3, from day 40), the concentrations of sodium acetate and sodium succinate were reduced to a C/N ratio of 3 in Ra and Rb. The effluent  $\text{NO}_3^-$  concentration fluctuated below 1  $\text{mg L}^{-1}$ , and the efficiencies of SR in Ra and Rb were reduced by 7.2% and 16.9%, respectively, compared to the previous stage. We suspect that this reduced efficiency of  $\text{SO}_4^{2-}$  removal was due to competition for electrons between  $\text{NO}_3^-$  and  $\text{SO}_4^{2-}$  at low C/N ratio. Dhamole *et al.*<sup>14</sup> studied denitrification employing acclimatized activated sludge in

a continuously stirred tank reactor at various C/N ratios ranging from 1.5 to 6. A C/N ratio of 2.00–2.25 was identified as most appropriate for denitrification under these experimental conditions. SRB is at a competitive disadvantage to DNB in nitrate and sulfate wastewater treatment, previous study<sup>15</sup> also found that the removal efficiency of sulfate decreased from 97.7% to 68.6% when the influent nitrate concentration increased from 1500 to 3500  $\text{mg L}^{-1}$ . To investigate the differences in the removal pathways of  $\text{NO}_3^-$  and  $\text{SO}_4^{2-}$  in reactors Ra and Rb, we carried out relevant batch experiments to demonstrate the effects of the different substrates on the intermediate products, as elaborated in Section 3.2.

### 3.2. Batch experiments

In order to thoroughly investigate the transformation during  $\text{NO}_3^-$  and  $\text{SO}_4^{2-}$  removal using sodium acetate and sodium succinate as substrates, batch experiments were carried out. This study was conducted at a C/N ratio of 5, at which the best removals of  $\text{NO}_3^-$  and  $\text{SO}_4^{2-}$  were achieved. Although both  $\text{NO}_3^-$  and  $\text{SO}_4^{2-}$  were reduced by the different substrates, the distributions of the resulting intermediates were slightly different. As shown in Fig. 3(a and c),  $\text{H}_2\text{S}$  (25  $\text{mg L}^{-1}$ ) and  $\text{NH}_4^+$  (5.94  $\text{mg L}^{-1}$ ) accumulated in reactor Ra, whereas almost no  $\text{H}_2\text{S}$  and  $\text{NH}_4^+$  accumulated in reactor Rb. The reduction of  $\text{NO}_3^-$  in reactor Ra was efficient, with a removal rate of 199.63  $\text{mg NO}_3^- \text{N (L h)}^{-1}$  over the first 3 h, giving a minimum effluent concentration of 1.1  $\text{mg L}^{-1}$ . Subsequently, due to the accumulation of  $\text{NH}_4^+$ , the denitrification pathway is inhibited, part of  $\text{NH}_4^+$  convert to the  $\text{NO}_3^-$  with concentration increased to 3.93  $\text{mg L}^{-1}$  by nitrification. The reduction of  $\text{SO}_4^{2-}$  was accomplished rapidly within the first 9 h, with a removal of 62.0%, but its concentration subsequently increased and exceeded that in the incoming water of 357.4  $\text{mg L}^{-1}$ . This may have been because the reaction proceeded late in the process, the DO in the system increased as the decreasing COD led to the regulation of sulfur-related biotransformation,<sup>26</sup> sulfides in Ra form sulfates in the presence of oxygen. The overall biological chemotrophic sulfur transformation reactions is described in eqn (3)–(7):



As shown in Fig. 3(a) and (b), SR in both reactors Ra and Rb proceeded rapidly in the first 9 h, accompanied by the accumulation of  $\text{H}_2\text{S}$  and  $\text{S}^0$  in Ra at levels of 25  $\text{mg L}^{-1}$  and 568.71  $\text{mg L}^{-1}$ , respectively. The  $\text{S}^{2-}$  concentration increased to

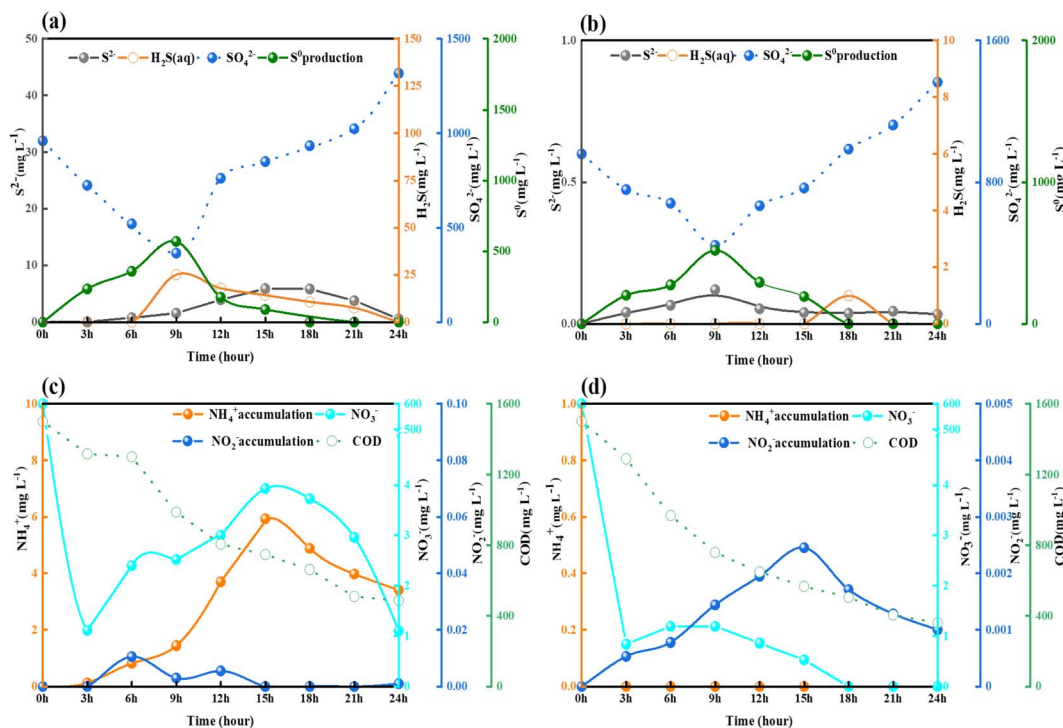


Fig. 3 Effects of different substrates on the conversion of  $\text{NO}_3^-$  and  $\text{SO}_4^{2-}$  removal: (a) Ra, (b) Rb, (c) Ra, and (d) Rb.

5.91  $\text{mg L}^{-1}$ , resulting in an  $\text{SO}_4^{2-}$  removal of 62.1% in Ra. Meanwhile, only slight  $\text{H}_2\text{S}$  and  $\text{S}^{2-}$  production was observed in Rb, amounting to less than 1  $\text{mg L}^{-1}$  and 0.13  $\text{mg L}^{-1}$ , respectively. Thus, the use of different substrates resulted in almost 25 times more  $\text{H}_2\text{S}$  being produced in Ra than in Rb.

Batch tests on denitrification revealed that accumulation of  $\text{NH}_4^+$  (5.94  $\text{mg L}^{-1}$ ) and the associated accumulation of nitrite (0.01  $\text{mg L}^{-1}$ ) in Ra also exceeded those in Rb. The accumulation of  $\text{NH}_4^+$  in the reactor clearly affected the reduction of  $\text{NO}_3^-$ , as shown in Fig. 3(c) and (d). It has been demonstrated in previous studies that  $\text{S}^{2-}$  metabolism and the mineralization of organic materials both caused SR, contributing to  $\text{NH}_4^+$  buildup.<sup>27,28</sup> Batch experiments have shown that intermediate product yields of nitrogen- and sulfur-related biotransformation are higher when sodium acetate is used as the carbon source compared to sodium succinate. The  $\text{S}^{2-}$  accumulated during SR in Ra not only contributes to the release of  $\text{H}_2\text{S}$  in the reaction compared to Rb, but also affects the conversion of  $\text{NO}_3^-$  through denitrification by the process of DNRA.  $\text{H}_2\text{S}$  increased from 0 to a peak of 25  $\text{mg L}^{-1}$  within 3 h in Ra, which prompted us to further explore the effect of different substrates on  $\text{NO}_3^-$  and  $\text{SO}_4^{2-}$  biotransformation.

### 3.3. EEM

Two representative pollutant types (protein-like and humic-acid-like substances) were identified in the reactors through visual inspection of three fluorescence peaks (Fig. 4): peak A (tryptophan-like,  $\lambda_{\text{ex}}/\lambda_{\text{em}} = 275/340 \text{ nm}$ ), peak B (fulvic-acid-like,  $\lambda_{\text{ex}}/\lambda_{\text{em}} = 300-370/400-500 \text{ nm}$ ), and peak C (tryptophan-like,  $\lambda_{\text{ex}}/\lambda_{\text{em}} = 275/340 \text{ nm}$ ).<sup>29,30</sup> EEM analysis showed that

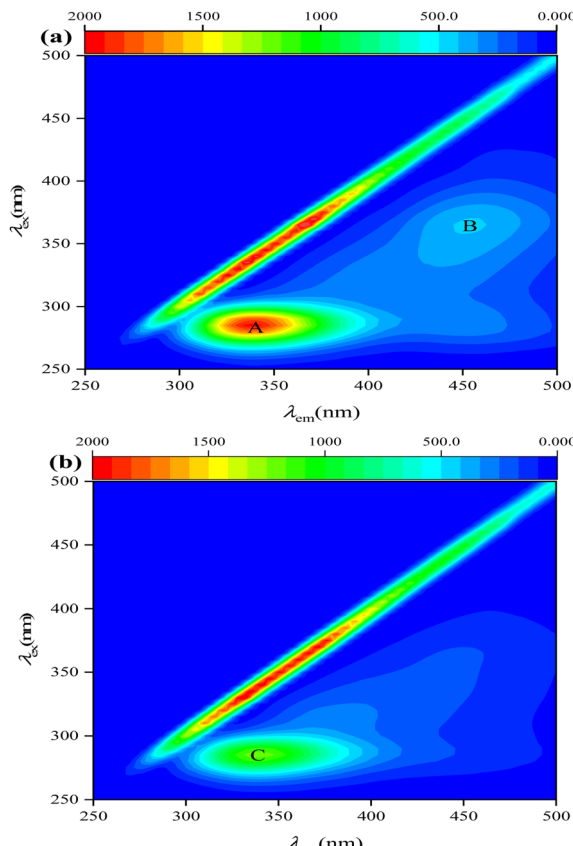


Fig. 4 EEM fluorescence spectra of the contents of Ra (a) and Rb (b).

tryptophan-like and fulvic-acid-like substances were present in Ra. In terms of fluorescence intensity, Ra produced more tryptophan- and fulvic-acid-like substances than Rb. Peaks A and C have an excitation wavelength of 275 nm and an emission wavelength of 340 nm, belonging to tryptophan-like and conventional T peaks. Peak B has  $\lambda_{\text{ex}}/\lambda_{\text{em}}$  maxima of 370/460 nm and can be assigned to the H peak, similar to terrestrial humus-like material from lignin and other terrestrial plants.<sup>31</sup> Peak T are closely related to the life activities of microorganisms. Thus, microbial biomass was more prevalent in the reactor when sodium acetate was used as the carbon source. This confirmed that intermediates such as  $\text{S}^{2-}$  and  $\text{NH}_4^+$  produced in Ra during  $\text{NO}_3^-$  and  $\text{SO}_4^{2-}$  removal were more abundant than in Rb due to more intense microbial activity.

### 3.4. Microbial community analysis in the system

We further determined the 16S rRNA-bacterial community structures within reactors Ra and Rb at various C/N ratios on the last day of each stage, aiming to explore the co-metabolic processes of the microbial community in the presence of different substrates. Ra1, Ra2, and Ra3 denote that sodium acetate was used as the carbon source in the reactor, and the C/N ratio was decreased from 8 to 5 to 3, respectively. Rb1, Rb2, and Rb3 denote that sodium succinate was used as the carbon source, and the C/N ratio was likewise decreased from 8 to 5 to 3. The Chao estimator, and the Shannon, Sobs, and Simpson indices, are shown in Table S2.† These indices are lower in Ra than in Rb, indicating a greater keystone taxa diversity in the latter. Based on pyrosequencing of the 16S rRNA gene, the bacterial communities differed between the two carbon sources according to phylogenetic classification, which supported denitrification and desulfurization systems at the phylum and genus levels (Fig. 5).

Most bacteria in the two reactors could be grouped into Proteobacteria, Firmicutes, Actinobacteriota, Bacteroidota, Desulfobacterota, Synergistota, and Patescibacteria. The bacteria in these phyla accounted for more than 90% of the total. It can be seen that Proteobacteria was the dominant phylum within the two reactors. The observation regarding Proteobacteria indicated that this phylum might play a significant functional role in the co-reduction of  $\text{SO}_4^{2-}$  and  $\text{NO}_3^-$ .<sup>15,32</sup> Ci *et al.* and Yang *et al.*<sup>33,34</sup> found the phyla Desulfobacterota and Firmicutes to play a vital role in the sulfur cycle, reducing  $\text{SO}_4^{2-}$  to  $\text{S}^{2-}$  using organic matter or  $\text{H}_2$ .<sup>35</sup> We observed a high abundance of Desulfobacterota (7.32%), which can utilize polysulfide, tetrathionate, or thiosulfate as electron acceptors<sup>36</sup> and may therefore be one of the reasons for the high  $\text{SO}_4^{2-}$  removal rate. Planctomycetota (9.6%), Latescibacteria (6.43%), Acidobacteriota (1.76%), and Dependentiae (1.16%) were more abundant in Rb.

Three primary functional groupings were found as the dominant populations of the culture at genus level in the two reactors, namely denitrifying bacteria (DNB), SRB, and DNRA bacteria. The highest abundance of *Thauera* was found in Ra, with the highest relative abundance in Ra3 (62.22%), much higher than in Rb3 (27.69%). *Thauera* is a typical denitrifying

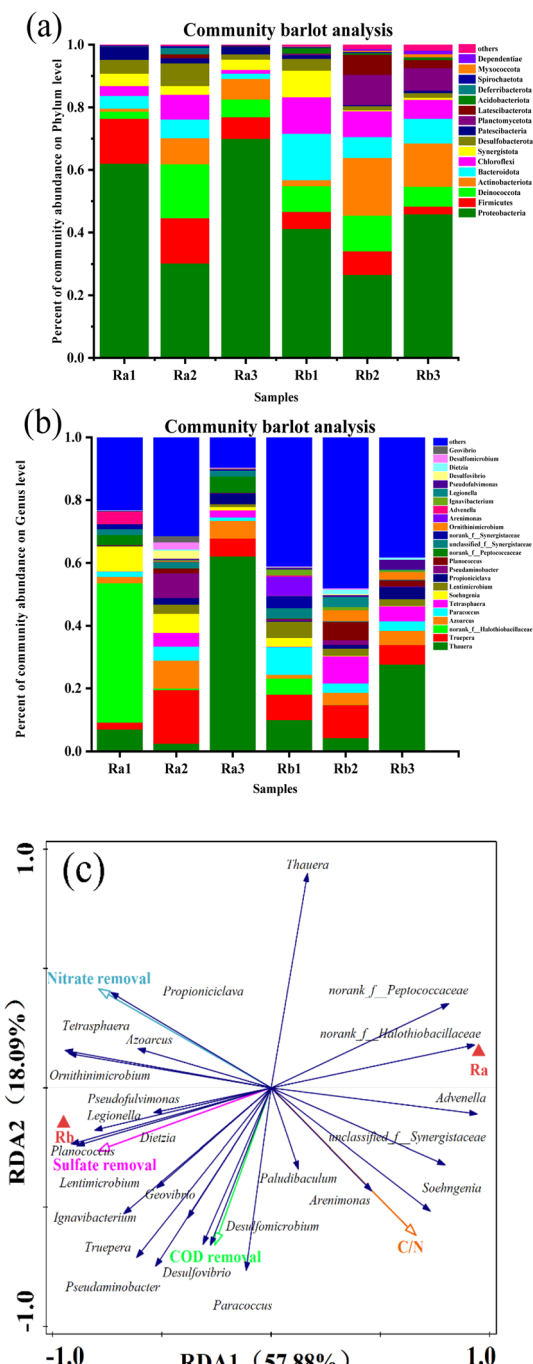


Fig. 5 Microbial community analysis: (a) phylum level and (b) genus level, and (c) radial distribution analysis (RDA).

bacterium that plays an important role in both denitrification and desulfurization, with organic materials acting as electron donors and carbon sources.<sup>8,37</sup> Moreover, *Azoarcus* and *Dietzia* are important facultative DNB.<sup>38,39</sup> *Azoarcus* was consistently more abundant in Ra (at up to 8.89%) than in Rb (at up to 4.55%). The fact that *Azoarcus* strains carry the *nar*, *nap*, *nir*, *nor*, and *nos* genes indicates that they might be able to obtain energy by anaerobic nitrate respiration; the majority of them are facultative anaerobes and diazotrophs.<sup>40</sup> *Paracoccus* is an



autotrophic denitrifying and desulfurizing microorganism, amounted to 4.46% and 8.82% in Ra and Rb, respectively. *Desulfomicrobium* (2.15%) and *Desulfovibrio* (2.6%) were identified as the dominant SRB in Ra. *Desulfomicrobium* has been reported to prefer H<sub>2</sub> as an electron donor for SR.<sup>41</sup> *Desulfovibrio* is an autotrophic DNRA bacterium that can utilize H<sub>2</sub> and S<sup>2-</sup> as electron donors to reduce NO<sub>3</sub><sup>-</sup> to NH<sub>4</sub><sup>+</sup>.<sup>42</sup>

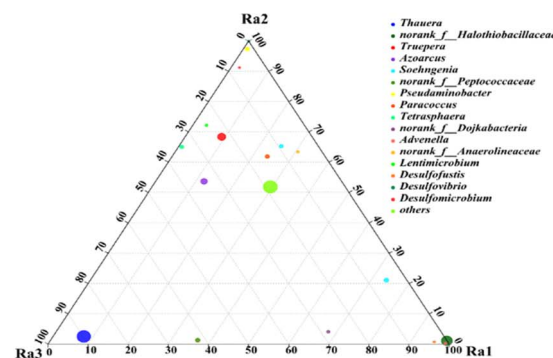
### 3.5. Variation in DO with different carbon sources and its effect on microbial community

We tested almost unmeasurable DO in the reactor, but the difference between Ra and Rb might be evidenced by the abundance of key taxa. At the phylum level, the abundance of Firmicute ranged from 6.8% to 14.34% in Ra, as compared to only 7.53% in Rb. Firmicute can remove NO<sub>3</sub><sup>-</sup> under anaerobic conditions. Higher NO<sub>3</sub><sup>-</sup> concentration and lower DO concentration in the initial water are conducive to increasing the abundance of Firmicutes in the raw aqueous biofilm system.<sup>43</sup> This may account for the lower DO level in Ra than in Rb. Bacteroidota is known to have an ability to degrade chemical organic nutrient polymers, which may contribute to the removal of COD from the reactor.<sup>44</sup> Given that COD was consumed relatively more quickly, the high enrichment level of Bacteroidota in Rb (14.8%) may be the cause of its slightly higher DO content. At the genus level, *Dietzia* is an aerobic denitrifying bacterium with a strong petroleum hydrocarbon degradation activity.<sup>45,46</sup> It was only enriched in Rb, with a relative abundance of more than 1%, consistent with the higher DO level in Rb. It can be deduced from the major microbial communities that the higher DO level in the system with sodium succinate as the carbon source is due to more rapid COD depletion.

### 3.6. Effect of different C/N ratios on microbial communities

As shown in Fig. 5(a), besides different substrates, various C/N ratios have different effects on microbial communities. At the phylum level, the relative abundances of Proteobacteria in the two reactors were lowest at a C/N ratio of 5, but much higher at a C/N ratio of 3, amounting to 30.22%/70.33% in Ra and 26.65%/45.90% in Rb. Ren *et al.*<sup>47</sup> found that a low C/N ratio increased the relative Proteobacteria content, which is favorable for denitrification. The dominant genera in the presence of different carbon sources (Ra and Rb) at different C/N ratios were clearly illustrated by ternary analysis (Fig. 6). Most of the dominant DNB appear in the region with Ra2 as the apex, such as *Paracoccus* and *Dietzia*, confirming that the microbial community conferred the best denitrification capacity in Ra2 at a C/N ratio of 5. *Desulfovibrio* and *Desulfomicrobium* were present at high levels in Ra2. Both DNB and SRB showed high abundance in Ra2, resulting in greater nitrogen and sulfur removal capacities, while a high level of *Thauera* (62.22%) was found in Ra3, and the amounts of other bacteria significantly decreased. In Rb, the highest abundance of *Thauera* (27.69%) was found at a C/N of 3. Most microorganisms were found in high abundance in Rb2 and Rb3, and similar trends were seen in both reactors, with *Azoarcus* and *Propioniciclavata* being more enriched at low C/N ratios. *Propioniciclavata* can utilize various

### Ternary analysis



### Ternary analysis

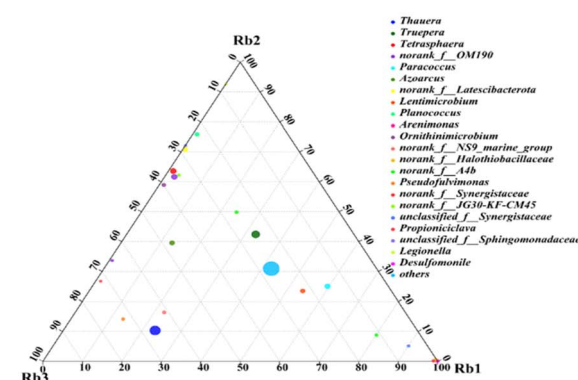


Fig. 6 Ternary analysis of Ra and Rb.

carbohydrates, including hexoses and disaccharides, to produce acetate and propionate.<sup>48</sup> *Paracoccus* was more enriched in Rb which is better adapted to high C/N ratios. The above observations imply that DNB function better at C/N ratios of 3. In contrast, SRB showed higher abundance at a C/N ratio of 5. Here, DB and SRB co-existed harmoniously in the respective reactors at a C/N ratio of 5.

### 3.7. Sulfate and nitrate reduction in the presence of different carbon sources

As shown in Fig. S1,<sup>†</sup> FAPROTAX functional prediction indicated that the abundance of functional genes predicted for SR was higher in Rb than in Ra at a C/N ratio of 8, and that the functional activity of denitrification was stronger than that of SR in both reactors. When the C/N ratio was decreased to 5, the denitrification and SR functions reached a relatively stable state, and in combination with the previous reactor performance, the removal of NO<sub>3</sub><sup>-</sup> and SO<sub>4</sub><sup>2-</sup> in the system reached an ideal state at this stage. Finally, the highest abundances of denitrification functions were predicted in Ra and Rb at a C/N ratio of 3, whereupon SR became greatly inhibited. Therefore, these predicted functional genes indicated that removal of NO<sub>3</sub><sup>-</sup> and SO<sub>4</sub><sup>2-</sup> at a C/N ratio of 5 was preferable.

In assessing the effect of different C/N ratios on NO<sub>3</sub><sup>-</sup> and SO<sub>4</sub><sup>2-</sup> removal, nitrate-reducing bacteria were seen to co-adapt



and co-metabolize with SRB. It has been demonstrated that *Paracoccus* displays some activity in the removal of  $\text{NO}_3^-$  and ammonia, with a preference for the latter.<sup>49,50</sup> In the first stage, the different abundances of *Paracoccus* in Ra (1.7%) and Rb (8.8%) may account for the competition between denitrification and DNRA. Luo *et al.*<sup>43</sup> demonstrated a positive correlation between *Actinobacteria* and  $\text{NH}_4^+$ , indicating that the growth of the former is crucial for accumulation of the latter. In this study, the highest accumulation of  $\text{NH}_4^+$  was observed at a C/N of 8, but the relative abundance of this bacterium was the lowest at 0.94%. Previous study has shown that high C/N ratio is one of the vital influencing factors affecting denitrification and the process of DNRA.<sup>51</sup> However, in the present study, this is contrary to the enrichment of  $\text{NH}_4^+$  in Ra. We speculate that it may be the  $\text{S}^{2-}$  generated in Ra as an electron donor and  $\text{NO}_3^-$  as an electron acceptor that produce  $\text{NH}_4^+$ . Thus, the presence of these microorganisms in Rb that can remove  $\text{NH}_4^+$  hinders the DNRA pathway.

The presence of higher DO levels in Rb than in Ra may affect the behavior of DNB and SRB in competing for electrons. First, batch experiments showed that more  $S^{2-}$  was produced in Ra and affected the reduction of  $NO_3^-$ . In contrast, no  $S^{2-}$  was accumulated in Rb. It is likely that the  $SO_4^{2-}$  in Ra was removed by anisotropic SR, whereas the  $SO_4^{2-}$  in Rb was removed by anabolic SR without  $S^{2-}$  accumulation. According to previous research, *Desulfomicrobium* prefers to employ  $H_2$  as an electron donor for SR.<sup>41</sup> *Desulfomicrobium* was enriched to 2.17% in Ra at C/N = 5. *Desulfovibrio* (2.6%) was observed exclusively in Ra. The relatively high concentration of  $S^{2-}$  in Ra might be more suitable for the growth of *Desulfovibrio*. Therefore, our study confirms that using sodium acetate as the carbon source is more suitable for the growth of some DNRA bacteria, whereas the greater keystone taxa diversity in Rb was shown by RDA (Fig. 5(c)), indicating a positive correlation with COD,  $NO_3^-$ , and  $SO_4^{2-}$  removal rates.

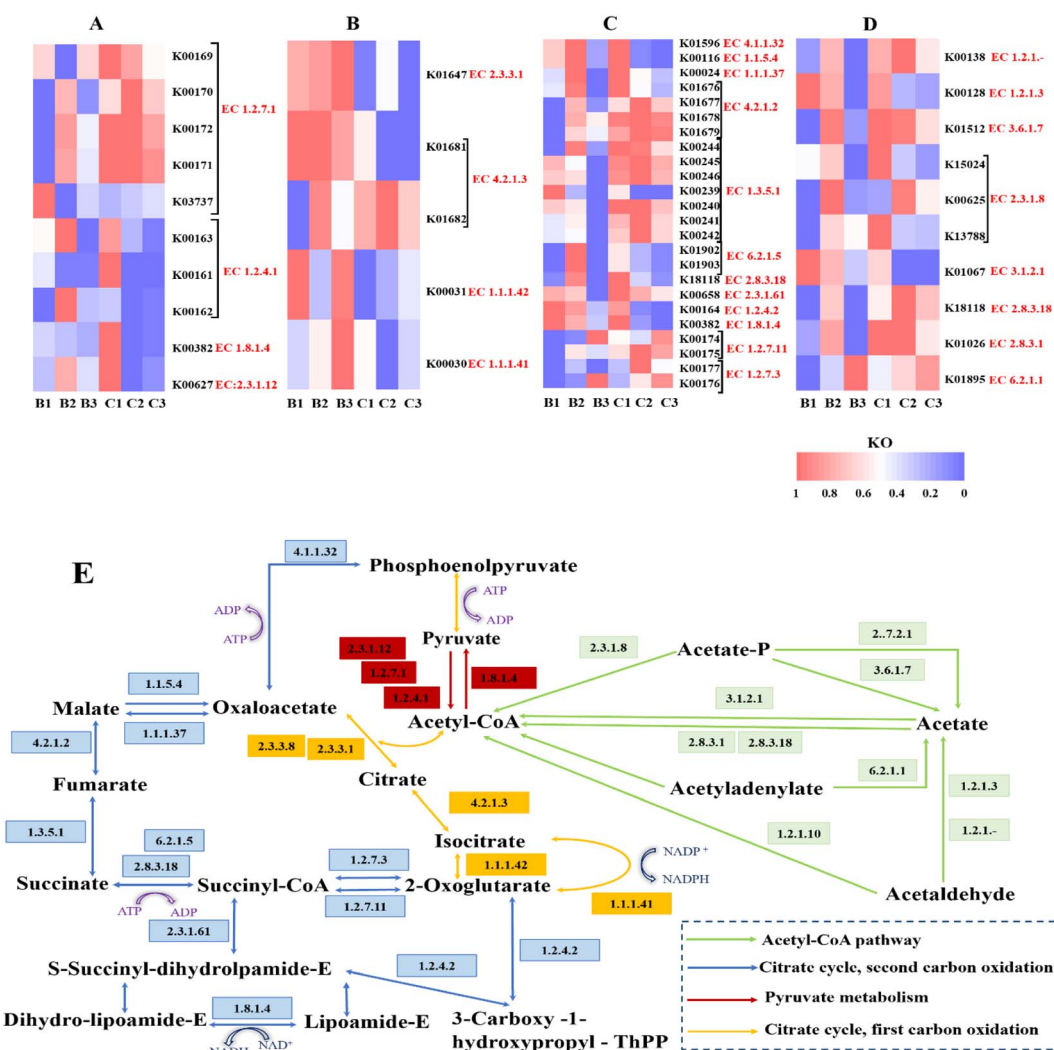


**Fig. 7** KEGG-based heat maps of the typical genes involved in the carbon metabolism process and their abundances: (A) pyruvate metabolism; (B) citrate cycle, first carbon oxidation; (C) citrate cycle, second carbon oxidation; (D) acetyl-CoA pathway. Based on the raw gene abundance data, unit variance normalization was applied. A red-colored block indicates a gene that is more abundant in that sample than in the other samples; a blue-colored block indicates a gene that is less abundant in that sample than in the other samples. (E) Potential mechanism of carbon metabolism of the two carbon sources in the respective reactors

### 3.8. Potential mechanisms of microbial activity on $\text{NO}_3^-$ , $\text{SO}_4^{2-}$ , and carbon substrates

The observed differences in the processes of  $\text{NO}_3^-$  and  $\text{SO}_4^{2-}$  reduction in the presence of different carbon sources motivated us to learn more about the potential mechanisms by which microorganisms in the system interact with the various substrates. Thus, the potential functional genes of microbial communities based on 16S rRNA gene sequence data were predicted by Phylogenetic Investigation of Communities by Reconstruction of Unobserved States (PICRUSt). In level 2 (metabolism), amino acid metabolism, carbohydrate metabolism, and energy metabolism were the main gene sequences (Table. S3†). Generally, acetate is directed to major metabolic pathways through acetyl co-enzyme A (acetyl-CoA), an activated form of acetate.<sup>52</sup> Acetyl-CoA and pyruvate are closely associated with regulation of the expression of genes regarding acetate metabolism. Meanwhile, the citrate cycle is directly related to succinate metabolism.<sup>53</sup> Thus, heat maps of the abundance of encoding genes for important enzymes in the three metabolic pathways were created in order to better understand the carbon metabolism routes of the two carbon sources (Fig. 7).

Fig. 7E illustrates the potential processes of carbon metabolism for the two carbon sources in accordance with the abundance of genes encoding key enzymes suggested by KEGG.

We have found that the second phase of the citrate cycle is enhanced at the C/N of 8 and that sodium succinate generates both succinate and acetate through the citrate cycle, second carbon oxidation, and the acetyl-CoA pathway. Synergistota can also produce short-chain fatty acids and consume acetate syntrophically.<sup>54</sup> Synergistota was consistently present in the different phases of Ra (2.7–3.93%). However, it was present at 8.41% in Rb during the first phase, but at less than 1% during the second phase. This implies that as the C/N ratio is decreased, Rb switches from using acetate derived from succinate to using succinate directly as a carbon source for metabolism. *Actinobacteria* showed a greater abundance in Rb (18.39%) than in Ra (8.37%). Relevant studies have confirmed that *Actinobacteria* have a more stable structure and higher adaptability than other microorganisms. *Planctomycetota* are comparatively slow-growing organisms with low carbon demand,<sup>55,56</sup> which were enriched at 9.6%/7.32% in the second and third stages of Rb, respectively, but were essentially non-existent in Ra. At the genus level, a peculiarity of *Lentimicrobium* is that it is both a carbohydrate fermenter and a denitrifier.<sup>57,58</sup> *Lentimicrobium* was more enriched in Rb (5.12%) than in Ra (2.93%), implying that sodium succinate might be more suitable as a fermentation carbon source and for denitrification in terms of simultaneous  $\text{NO}_3^-$  and  $\text{SO}_4^{2-}$  removal. On the other hand, the carbon metabolism of sodium acetate has been shown to be significantly improved at a C/N ratio of 5, and we have observed a high prevalence of the first stage of the citrate cycle at the C/N ratio of 5 in Ra.

## 4 Conclusions

Differences in  $\text{NO}_3^-$  and  $\text{SO}_4^{2-}$  co-removal in the presence of different substrates have been investigated. It was found that

the best co-removal of  $\text{NO}_3^-$  and  $\text{SO}_4^{2-}$  in the two systems was achieved at a C/N ratio of 5, and that sodium acetate as a carbon source produced more  $\text{H}_2\text{S}$  and  $\text{S}^{2-}$  than sodium succinate, which regulated the biotransformation of  $\text{NO}_3^-$  from denitrification to DNRA. As a carbon source, sodium succinate does not produce  $\text{H}_2\text{S}$ , which can reduce secondary pollution. Different carbon sources led to different microbial community structures, with sodium succinate eliciting a great taxa diversity and a more stable microbial community. The potential carbon metabolic pathways of the two carbon sources have been further revealed. Our results imply that sodium succinate generates both succinate and acetate through the citrate cycle and acetyl-CoA pathway. The carbon metabolism of sodium acetate is significantly improved at a C/N ratio of 5. This study provides a research basis for the treatment of actual industrial wastewater containing  $\text{NO}_3^-$  and  $\text{SO}_4^{2-}$ . However, there is big difference between actual wastewater and synthetic wastewater. Experimental results with synthetic wastewater have limitations to be applied to actual conditions. New approaches for the simultaneous removal of  $\text{NO}_3^-$  and  $\text{SO}_4^{2-}$  in the presence of various substrates are anticipated to emerge from this study, and further analysis is still needed to delineate more detailed differences in carbon metabolism.

## Author contributions

Baixiang Wang: conceptualization, methodology, formal analysis, data curation, writing – original draft. Heping Hu: writing – review & editing. Haiguang Yuan: writing – review & editing. Yanlin Wang: writing – review & editing. Zerui Gong: methodology, visualization, investigation. Xinyue Xu: data curation, investigation. Tianyu Zhao: resources. Shaobin Huang: conceptualization, supervision, funding acquisition.

## Conflicts of interest

The authors declare that they have no known competing financial interests or personal relationships that could have appeared to influence the work reported in this paper.

## Acknowledgements

This work is financially supported by National Natural Science Foundation of China (No. 52270105), Science and Technology Innovation Program from Water Resources of Guangdong Province (No. 2023-03) and China Water Resources Pearl River Planning Surveying & Designing Co. Ltd.

## References

- 1 M. D. Krom, A. Ben David, E. D. Ingall, L. G. Benning, S. Clerici, S. Bottrell, C. Davies, N. J. Potts, R. J. Mortimer and J. van Rijn, *Water Res.*, 2014, **56**, 109–121.
- 2 Q. Li, B. Huang, X. Chen and Y. Shi, *Water Res.*, 2015, **75**, 33–42.
- 3 L. Zhang, G. Fu and Z. Zhang, *Bioresour. Technol.*, 2019, **289**, 121630.



4 M. H. Cai, G. Luo, J. Li, W. T. Li, Y. Li and A. M. Li, *Chemosphere*, 2021, **280**, 130937.

5 A. Ansari, E. T. Nadres, M. Dô and D. F. Rodrigues, *Process Saf. Environ. Prot.*, 2021, **150**, 365–372.

6 Y. Fernandez-Nava, E. Maranon, J. Soons and L. Castrillon, *J. Hazard. Mater.*, 2010, **173**, 682–688.

7 C. Chen, L. Liu, D. J. Lee, W. Guo, A. Wang, X. Xu, X. Zhou, D. Wu and N. Ren, *Bioresour. Technol.*, 2014, **155**, 161–169.

8 C. Huang, Y. Zhao, Z. Li, Y. Yuan, C. Chen, W. Tan, S. Gao, L. Gao, J. Zhou and A. Wang, *Bioresour. Technol.*, 2015, **192**, 478–485.

9 H. K. Carlson, M. K. Stoeva, N. B. Justice, A. Sczesnak, M. R. Mullan, L. A. Mosqueda, J. V. Kuehl, A. M. Deutschbauer, A. P. Arkin and J. D. Coates, *Environ. Sci. Technol.*, 2015, **49**, 3727–3736.

10 E. A. Greene, a. G. Voordouw, C. Hubert and G. E. J. M. Nemati, *Environ. Microbiol.*, 2003, **7**, 607–617.

11 J. Garcia-de-Lomas, A. Corzo, M. Carmen Portillo, J. M. Gonzalez, J. A. Andrades, C. Saiz-Jimenez and E. Garcia-Robledo, *Water Res.*, 2007, **41**, 3121–3131.

12 X. Xu, C. Chen, A. Wang, W. Guo, X. Zhou, D. J. Lee, N. Ren and J. S. Chang, *J. Hazard. Mater.*, 2014, **264**, 16–24.

13 A. Ontiveros-Valencia, M. Ziv-El, H. P. Zhao, L. Feng, B. E. Rittmann and R. Krajmalnik-Brown, *Environ. Sci. Technol.*, 2012, **46**, 11289–11298.

14 P. B. Dhamole, R. R. Nair, S. F. D'Souza, A. B. Pandit and S. S. Lele, *Appl. Biochem. Biotechnol.*, 2015, **175**, 748–756.

15 C. Chen, X. J. Xu, P. Xie, Y. Yuan, X. Zhou, A. J. Wang, D. J. Lee and N. Q. Ren, *Chemosphere*, 2017, **171**, 294–301.

16 C. Chen, R. C. Zhang, X. J. Xu, N. Fang, A. J. Wang, N. Q. Ren and D. J. Lee, *Bioresour. Technol.*, 2017, **232**, 417–422.

17 L. Yang, Y.-X. Ren, S.-Q. Zhao, X. Liang and J.-p. Wang, *Ann. Microbiol.*, 2015, **66**, 737–747.

18 E. M. van den Berg, U. van Dongen, B. Abbas and M. C. van Loosdrecht, *ISME J.*, 2015, **9**, 2153–2161.

19 Y. You, S. Chu, M. Khalid, K. Hayat, X. Yang, D. Zhang and P. Zhou, *J. Cleaner Prod.*, 2022, **346**, 131169.

20 R. R. Nair, P. B. Dhamole, S. S. Lele and S. F. D'Souza, *Chemosphere*, 2007, **67**, 1612–1617.

21 S. Gao, Z. Li, Y. Hou, A. Wang, Q. Liu and C. Huang, *Environ. Res.*, 2022, **204**, 111946.

22 Y. Wang, J. Li, S. Huang, X. Huang, W. Hu, J. Pu and M. Xu, *J. Hazard. Mater.*, 2021, **415**, 125741.

23 C. Sun, J. Yuan, H. Xu, S. Huang, X. Wen, N. Tong and Y. Zhang, *Bioresour. Technol.*, 2019, **290**, 121768.

24 Y. Zhao, Q. Li, Q. Cui and S.-Q. Ni, *Chem. Eng. J.*, 2022, **441**, 135938.

25 Y. Hu, Z. Jing, Y. Sudo, Q. Niu, J. Du, J. Wu and Y. Y. Li, *Chemosphere*, 2015, **130**, 24–33.

26 Z. Qian, H. Tianwei, H. R. Mackey, M. C. M. van Loosdrecht and C. Guanghao, *Water Res.*, 2019, **150**, 162–181.

27 J. J. Wright, K. M. Konwar and S. J. Hallam, *Nat. Rev. Microbiol.*, 2012, **10**, 381–394.

28 D. E. Canfield, F. J. Stewart, B. Thamdrup, L. De Brabandere, T. Dalsgaard, E. F. Delong, N. P. Revsbech and O. Ulloa, *Science*, 2010, **330**, 1375–1378.

29 K. Lu, H. Gao, H. Yu, D. Liu, N. Zhu and K. Wan, *Sci. Total Environ.*, 2022, **816**, 151531.

30 J. He, X. Wu, G. Zhi, Y. Yang, L. Wu, Y. Zhang, B. Zheng, A. Qadeer, J. Zheng, W. Deng, H. Zhou and Z. Shao, *Ecol. Indic.*, 2022, **142**, 109088.

31 L. Yan, Q. Liu, C. Liu, Y. Liu, M. Zhang, Y. Zhang, Y. Zhang and W. Gu, *Ecotoxicol. Environ. Saf.*, 2019, **184**, 109616.

32 X.-J. Xu, C. Chen, X. Guan, Y. Yuan, A.-J. Wang, D.-J. Lee, Z.-F. Zhang, J. Zhang, Y.-J. Zhong and N.-Q. Ren, *Chem. Eng. J.*, 2017, **330**, 63–70.

33 B. Yang, Y. Wang, Y. Lu, L. Liu, S. Huang, F. Cheng and Z. Feng, *J. Water Process. Eng.*, 2022, **47**, 102737.

34 M. Ci, W. Yang, H. Jin, L. Hu, C. Fang, D. Shen and Y. Long, *Waste Manage.*, 2022, **141**, 52–62.

35 T. L. Hamilton, R. J. Bovee, S. R. Sattin, W. Mohr, W. P. Gilhooley 3rd, T. W. Lyons, A. Pearson and J. L. Macalady, *Front. Microbiol.*, 2016, **7**, 598.

36 C. L. Murphy, J. Biggerstaff, A. Eichhorn, E. Ewing, R. Shahan, D. Soriano, S. Stewart, K. VanMol, R. Walker, P. Walters, M. S. Elshahed and N. H. Youssef, *Environ. Microbiol.*, 2021, **23**, 4326–4343.

37 K. Zhang, L. Song and X. Dong, *Int. J. Syst. Evol. Microbiol.*, 2010, **60**, 2221–2225.

38 N. Yang, G. Zhan, D. Li, X. Wang, X. He and H. Liu, *Chem. Eng. J.*, 2019, **356**, 506–515.

39 S. Deng, S. Peng, B. Xie, X. Yang, S. Sun, H. Yao and D. Li, *Chem. Eng. J.*, 2020, **393**, 124736.

40 R. T. Raittz, C. Reginatto De Pierri, M. Maluk, M. Bueno Batista, M. Carmona, M. Junghare, H. Faoro, L. M. Cruz, F. Battistoni, E. Souza, F. O. Pedrosa, W. M. Chen, P. S. Poole, R. A. Dixon and E. K. James, *Genes*, 2021, **12**, 71.

41 H. Luo, J. Bai, J. He, G. Liu, Y. Lu, R. Zhang and C. Zeng, *Sci. Total Environ.*, 2020, **728**, 138685.

42 S. Xu, X. Wu and H. Lu, *Front. Environ. Sci. Eng.*, 2021, **15**, 6.

43 J. Luo, H. Liang, L. Yan, J. Ma, Y. Yang and G. Li, *Bioresour. Technol.*, 2013, **148**, 189–195.

44 H. Stevens, M. Stubner, M. Simon and T. Brinkhoff, *FEMS Microbiol. Ecol.*, 2005, **54**, 351–365.

45 S. Yang, M. Yu and J. Chen, *Braz. J. Microbiol.*, 2017, **48**, 393–394.

46 V. Mendez, S. Holland, S. Bhardwaj, J. McDonald, S. Khan, D. O'Carroll, R. Pickford, S. Richards, C. O'Farrell, N. Coleman, M. Lee and M. J. Manefield, *Sci. Total Environ.*, 2022, **829**, 154587.

47 J. Ren, W. Cheng, M. Jiao, T. Meng, T. Lv and F. Liu, *J. Environ. Chem. Eng.*, 2022, **10**, 107585.

48 Y. Sugawara, A. Ueki, K. Abe, N. Kaku, K. Watanabe and K. Ueki, *Int. J. Syst. Evol. Microbiol.*, 2011, **61**, 2298–2303.

49 L. Zheng, Y. Dong, B. Li, T. Yin, C. Liu and H. Lin, *Bioresour. Technol.*, 2022, **359**, 127457.

50 B. Yang, Y. Qin, X. He, H. Li and J. Ma, *Sci. Total Environ.*, 2022, **810**, 152236.

51 X. Li, Q. Deng, Z. Zhang, D. Bai, Z. Liu, X. Cao, Y. Zhou and C. Song, *Chemosphere*, 2022, **308**, 136385.

52 Y. Kim, S. Lama, D. Agrawal, V. Kumar and S. Park, *Biotechnol. Adv.*, 2021, **49**, 107736.



53 R. Wan, L. Wang, Y. Chen, X. Zheng, J. Chew and H. Huang, *Water Res.*, 2019, **162**, 190–199.

54 D. Riviere, V. Desvignes, E. Pelletier, S. Chaussonnerie, S. Guermazi, J. Weissenbach, T. Li, P. Camacho and A. Sghir, *ISME J.*, 2009, **3**, 700–714.

55 S. L. S. Rollemburg, L. Q. de Oliveira, A. R. M. Barros, V. M. M. Melo, P. I. M. Firmino and A. B. Dos Santos, *Bioresour. Technol.*, 2019, **278**, 195–204.

56 V. E. P. S. G. da Silva, S. L. d. S. Rollemburg and A. B. dos Santos, *Process Saf. Environ. Prot.*, 2023, **171**, 1031–1042.

57 L. Sun, M. Toyonaga, A. Ohashi, D. M. Tourlousse, N. Matsuura, X. Y. Meng, H. Tamaki, S. Hanada, R. Cruz, T. Yamaguchi and Y. Sekiguchi, *Int. J. Syst. Evol. Microbiol.*, 2016, **66**, 2635–2642.

58 H. Wang, N. Chen, C. Feng, Y. Deng and Y. Gao, *Chemosphere*, 2020, **253**, 126693.

